

1 NASA-TM-82813

NASA Technical Memorandum 82813

NASA-TM-82813 19820013730

82N21604

# Coupled Bending-Bending-Torsion of a Mistuned Cascade With Nonuniform Blades

Krishna Rao V. Kaza  
*The University of Toledo*  
*Toledo, Ohio*

and

Robert E. Kielb  
*Lewis Research Center*  
*Cleveland, Ohio*

LIBRARY COPY

AUG 1 0 1988

LANGLEY RESEARCH CENTER  
LIBRARY NASA  
HAMPTON, VIRGINIA

Prepared for the  
Twenty-third Structures, Structural Dynamics and Materials Conference  
cosponsored by the AIAA, ASME, ASCE, and AHS  
New Orleans, Louisiana, May 10-12, 1982



COUPLED BENDING-BENDING-TORSION FLUTTER OF A  
MISTUNED CASCADE WITH NONUNIFORM BLADES

Krishna Rao V. Kaza\*

The University of Toledo  
Toledo, Ohio 43606 and

National Aeronautics and Space Administration  
Lewis Research Center  
Cleveland, Ohio 44135

and

Robert E. Kielb\*\*

National Aeronautics and Space Administration  
Lewis Research Center  
Cleveland, Ohio 44135

Abstract

A set of aeroelastic equations describing the motion of an arbitrarily mistuned cascade with flexible, pretwisted, nonuniform blades is developed using an extended Hamilton's principle. The derivation of the equations has its basis in the geometric nonlinear theory of elasticity in which the elongations and shears are negligible compared to unity. A general expression for foreshortening of a blade is derived and is explicitly used in the formulation. The blade aerodynamic loading in the subsonic and supersonic flow regimes is obtained from two-dimensional, unsteady, cascade theories. The aerodynamic, inertial and structural coupling between the bending (in two planes) and torsional motions of the blade is included. The equations are used to investigate the aeroelastic stability and to quantify the effect of frequency mistuning on flutter in turbofans. Results indicate that a moderate amount of intentional mistuning has enough potential to alleviate flutter problems in unshrouded, high-aspect-ratio turbofans.

Nomenclature

A cross sectional area of the blade  
 $A_0$  reference value of A  
 $[A], [A_r]$  aerodynamic matrices  
 $A_j$  torsional mode shape  
 $a$  elastic axis location  
 $a_0$  speed of sound  
 $B_1, B_2$  blade sectional constants  
 $b, b_R$  semichord and reference semichord  
 $c$  blade chord  
 $E$  Young's modulus of elasticity  
 $[E], [\bar{E}_{s,r}]$  matrices  
 $e$  mass and elastic axis offset (also base for natural logarithm)

$e_A$

$\bar{e}_x, \bar{e}_y, \bar{e}_z$   
 $\bar{e}_{x_3}, \bar{e}_{y_3}, \bar{e}_{z_3}$

G

$\bar{g}_{si}, \bar{h}_{si}$

$\bar{g}_{ari}, \bar{h}_{ari}$

$I_{xx}, I_{zz}$

$I_{xx0}$

[1]

i

J

$J_0$

k

$k_m$

$k_{m0}$

area centroid and elastic axis offset

unit vectors along x,y,z axes

unit vectors along  $x_3, y_3, z_3$  axes

shear modulus of elasticity

nondimensional amplitudes of

generalized coordinates

associated with the bending

modes  $W_i$  of the sth

blade measured out of and in

the plane of rotation

nondimensional amplitudes of

generalized coordinates

associated with the bending

modes  $W_i$  in the rth mode

of a tuned cascade

bending moment of inertia

about the major (parallel

to the x-axis) and minor

axis through centroid

reference bending moment of

inertia

unity matrix

$\sqrt{-1}$

torsional stiffness constant

reference value for J

reduced frequency,  $\omega_0 b / V_{eff} =$

$\omega_0 b / M_{eff} a_0$

polar mass radius of gyration

about elastic axis

$(k_m^2 = k_{m1}^2 + k_{m2}^2)$

reference polar radius of

gyration of cross sectional

mass about elastic axis

E-1156

\*Adjunct Professor, Mechanical Engineering Department, Associate Fellow, AIAA.

\*\*Aerospace Engineer, Structures Branch, Member AIAA.

N82-21604#

$k_{m_1}, k_{m_2}$	mass radii of gyration about x and z axes	$r_{a_0}$	reference radius of gyration
$k_A$	polar radii of gyration of cross-sectional area about elastic axis	$r_0, r_1$	running blade coordinate along elastic axis before and after deformation
L	blade length	$\bar{r}_0, \bar{r}_1$	position vector of an arbitrary point on the blade before and after deformation, Eqs. (A6) and (A7)
$L_a$	lift per unit span, positive up (negative z direction)	$\bar{R}_0, \bar{R}_1$	position vector of a point on elastic axis before and after deformation, Eqs. (A6) and (A7)
$L_{hhrij}, \dots, L_{\alpha\alpha rij}$	aerodynamic coefficients, in the rth mode of cascade	$S_{hhsij}, \dots, S_{\alpha\alpha sij}$	stiffness coefficients of the sth blade
$l_{hhr}, l_{har}$	nondimensional lift coefficients due to bending and torsional motions in the rth cascade mode	[S], [S <sub>s</sub> ]	stiffness matrices
$l_{ahr}, l_{aar}$	nondimensional moment coefficients due to bending and torsional motion in the rth cascade mode	s	integer specifying blade, s = 0, 1, 2, N-1; also blade spacing
$M_{ax}$	axial Mach number, $V_a/a_0$	$T_k$	kinetic energy
$M_a$	aerodynamic moment per unit span about the elastic axis, positive nose up	$T_c, \bar{T}_c$	blade tension, $\bar{T}_c = T_c/m_0 \omega^2 L^2$
$M_r$	relative Mach number, $\sqrt{V_a^2 + \omega^2 r^2}/a_0$	[T]	transformation matrix
$M_{eff}$	effective relative Mach number, $V_{eff}/a_0$	t, t <sub>0</sub> , t <sub>1</sub>	time, initial time, final time
$M_g, M_h, M_\alpha$	number of generalized coordinates with the bending motions out of and in the plane of rotation and with the torsional motion	U	strain energy
$M_{hhsij}, \dots, M_{\alpha\alpha sij}$	inertial coefficients of the sth blade	U <sub>F</sub>	radial foreshortening
[M], [M <sub>s</sub> ]	inertial matrices	u, v, w	deformations of elastic axis in $X_\Omega, Y_\Omega$ and $Z_\Omega$ directions
m	mass per unit length	$v_a$	axial velocity
$m_0$	reference mass per unit length	$v_{eff}$	effective relative velocity, $\sqrt{V_a^2 + \omega^2 r^2} \cdot \cos[90 - \xi - \tan^{-1}(V_a/\omega r)]$
N	number of blades in cascade	$v_e$	axial extension of elastic axis
P, P'	an arbitrary point on the elastic axis before and after deformation	W	work done by aerodynamic loading
[P]	stiffness matrix, Eq. (16)	$W_i$ (i = 1, 2, ...)	beam functions
$P_j$	quantity defined by Eq. (4)	[W], [W]	model function matrices
[Q]	matrix, Eq. (16)	$X_\Omega, Y_\Omega, Z_\Omega$	hub-fixed axis system, rotates about the $Z_\Omega$ -axis with an angular velocity $\omega$
$R_H$	hub radius	xyz	blade fixed axis system at arbitrary point on elastic axis
$R_T$	blade tip radius	$x_3 y_3 z_3$	blade fixed axis system in the deformed configuration obtained by rotating xyz
r	integer (0, 1, 2, ... N-1) specifying mode of a tuned cascade; also blade coordinate along elastic axis before deformation	{X <sub>s</sub> }, {X}	column matrices
		{Y <sub>r</sub> }, {Y}	column matrices

$\alpha$	angle of twisting deformation, positive when leading edge is upward
$\alpha_{si} \ (i = 1, 2, \dots)$	amplitudes of generalized coordinates associated with torsional modes $A_i$ of the $s$ th blade
$\alpha_{ari}$	amplitudes of generalized coordinates associated with torsional modes $A_i$ in the $r$ th mode of tuned cascade
$\beta_r$	interblade phase angle in the $r$ th mode of tuned cascade, $2\pi r/N$
$\gamma$	nondimensional eigenvalue, $(\omega/\omega_0)^2$
$\gamma_{yy}, \gamma_{yx}, \gamma_{yz}$	engineering strain components
$\delta(\ )$	variation of ( )
$\epsilon_{yy}, \epsilon_{yx}, \epsilon_{yz}$	tensor strain components
$\zeta_{hs1}, \dots, \zeta_{as1}$	damping ratios of $s$ th blade
$\eta, \bar{\eta}, \eta_a$	blade running coordinate measured from hub; $\bar{\eta} = \eta/L$ ; blade elastic axis position; $\eta_a = (a + 1)/2$
$\mu_0$	reference mass ratio, $m_0/\pi\rho_a b^2 R$
$\bar{\mu}$	real part of eigenvalue
$\xi$	pretwist angle
$\rho_a, \rho_m$	fluid and blade material density
$\tau$	nondimensional time, $t\omega_0$
$\bar{\nu}$	imaginary part of eigenvalue
$\Omega$	rotational speed
$\omega, \omega_0$	frequency and reference frequency
$\bar{\omega}$	angular velocity vector expressed in xyz system
$\bar{\omega}_{xyz}, \bar{\omega}_{x_3y_3z_3}$	curvature vectors
$(\dot{\ })$	derivative $a(\ )/at$ or $a(\ )/\partial\tau$
$(\prime)$	derivative $a(\ )/ar$ or $a(\ )/\partial\eta$

### 1. Introduction

A research program in propulsion system aeroelasticity is being conducted at the NASA Lewis Research Center. As a part of this general program, an effort was made by the authors in Refs. 1 and 2, to improve the physical understanding of turbofan engine aeroelastic characteristics including blade mistuning (nonidentical blade properties) effects. Other published work on mistuning was cited in Refs. 1 and 2.

The mathematical formulation considered in Ref. 1 is a 'typical section' model with two degrees of freedom, a bending and a pitching about the elastic axis. This model was found to be sufficient to elicit physical understanding of mistuning effects and to conduct parametric studies. Furthermore, this model was utilized in Ref. 3 to show that mistuning has enough potential to significantly raise the flutter speed of an advanced fan. This potential may have a very practical significance in eliminating the commonly used midspan shrouds in advanced turbofan designs. The main purpose of the midspan shrouds is to increase the blade natural frequencies and thus to avoid aeroelastic instabilities. However, the shrouds have an adverse effect on aerodynamic performance.

While the typical section model served the intended purposes, it is expected to be inadequate to obtain accurate flutter boundaries of modern technology turbofans or advanced turboprop blades which have a considerable amount of pretwist. As a consequence of pretwist, bending out of the plane of rotation couples elastically with bending in the plane of rotation. Consequently, a more realistic structural model of a blade is required.

The purposes of the research summarized in this paper are: (1) to develop a more refined and realistic structural model of a blade than the typical section model and to combine this model with the available unsteady cascade aerodynamic models; and (2) to study the effects of mistuning and other cascade parameters on flutter characteristics of an advanced technology fan stage. To the best of authors' knowledge, the mentioned effects utilizing the proposed model have not been studied in the published literature.

There exist several levels of approximations in structural theory used in rotary wing aeroelasticity to represent a structural model of a blade. The theory of pretwisted blades presented in Ref. 4 may be viewed as the first level of approximation. The structural theories presented in Refs. 5-9 may be viewed as ones with the second level of approximation. Since the corresponding unsteady cascade aerodynamic theory consistent with the second level structural theories is not available, the theory of Ref. 4 is used as a first step.

The governing equations of motion of a rotating, pretwisted blade are derived by using an extended Hamilton's principle. The derivation is characterized by the use of an axial (along the beam axis) displacement which includes second-degree nonlinear terms defining the axial foreshortening<sup>10</sup> of the tension axis due to bending, torsion, and the noncoincidence of the elastic axis and tension axis. The development of a more general expression for foreshortening than that used in Ref. 10 and the explicit use of this general expression in the axial displacement field are believed to be new. The explicit consideration of foreshortening in deriving the equations is appealing in that it parallels the corresponding development of equations for a nonrotating blade where retention of second-degree terms in the kinetic and potential energy expressions leads to linear equations (See Ref. 10). A more detailed discussion on the role of the general expression for foreshortening in deriving the second-degree nonlinear equations of motion and in accounting for the geometric stiffness effects in beam analyses

using finite-element methods will be presented in a future publication. The disk is assumed to be rigid. The unsteady, two-dimensional, cascade, aerodynamic loads are calculated by Smith's theory<sup>11</sup> in subsonic flow and Adamczyk and Goldstein's theory<sup>12</sup> in supersonic flow with a subsonic leading edge. The governing equations of motion of a mistuned cascade are formulated by assuming that the general motion of a blade is a linear combination of its motions in all possible modes of a tuned cascade. The space variable in the coupled integro-partial differential equations of motion is eliminated by using a modified Galerkin's method. The resulting equations are cast as a standard complex eigenvalue problem from which the aeroelastic stability is determined.

A digital computer program is developed to form and solve the complex eigenvalue problem. This program is written in a modular form such that it can be applied to advanced turboprops, helicopter rotors in hover, and wind turbine rotors by incorporating the appropriate aerodynamic modules. Due to length constraints of the paper, limited results are presented only for an advanced turbofan blade. However, additional parametric results will be presented in a future publication.

## II. Theory

The components of a bladed disk system have complex geometries. The analysis of this system is further complicated by blade mistuning. To investigate the aeroelastic stability of a cascade with mistuning, a mathematical model will be developed in this section.

### A. Coordinate Systems

Several coordinate systems will be employed in the derivation of equations of motion; those which are common to both the structural and aerodynamic aspects of the derivation for the *s*th blade are shown in Figs. 1 and 2. The axis system  $X_\Omega Y_\Omega Z_\Omega$  shown in the figures rotates with a constant angular velocity  $\Omega$  about the  $X_\Omega$ -axis. The  $Y_\Omega$ -axis coincides with the undeformed elastic axis of the blade. The blade principal axes,  $x$  and  $z$ , of the cross section at an arbitrary point on the elastic axis are inclined to the  $X_\Omega$  and  $Z_\Omega$  axes by an angle  $\xi$  as shown in Fig. 2. The blade elastic deformations,  $u$ ,  $v$ ,  $w$ , and  $\alpha$  translate and rotate the  $xyz$  system to the  $x_3y_3z_3$  system as shown in Fig. 1.

### B. Tuned Cascade Model

If the blades are tuned, the  $N$ -bladed cascade has  $N$  interblade phase angle modes with a constant phase angle  $\beta_r$  between adjacent blades. This interblade phase angle is restricted by Lane's<sup>13</sup> assumption to the  $N$  discrete values  $\beta_r = 2\pi r/N$  where  $r = 0, 1, 2, \dots, N-1$ . In each of these modes all blades have the same amplitude. For a tuned cascade, the modes with different interblade phase angles are uncoupled. The blade deflections are expressed in a traveling wave form in terms of a set of generalized coordinates which are associated with the nonrotating uncoupled beam modes in pure bending and torsion. The number of modes retained in the plane of rotation, in the plane perpendicular to the plane of rotation, and in torsion are  $M_h$ ,  $M_g$ , and  $M_\alpha$  respectively. The blade deflections expressed in traveling wave form are

$$\begin{Bmatrix} w/b_R \\ u/b_R \\ \alpha \end{Bmatrix} = [\bar{W}] \{X_s\} e^{i \frac{\omega}{\omega_0} \tau} = [\bar{E}_{s,r}] [\bar{W}] \{Y_r\} e^{i \frac{\omega}{\omega_0} \tau} \quad (1)$$

where

$$[\bar{W}] = \begin{bmatrix} W_1 & W_2 & \dots & 0 & 0 \\ 0 & 0 & \dots & W_1 & W_2 & \dots \\ 0 & 0 & \dots & 0 & 0 & \dots & A_1, A_2, \dots \end{bmatrix}$$

$$\{X_s\} = \{\bar{h}_{s1} \bar{h}_{s2} \dots \bar{g}_{s1} \bar{g}_{s2} \dots \alpha_{s1} \alpha_{s2} \dots\}^T$$

$$\{Y_r\} = \{\bar{h}_{ar1} \bar{h}_{ar2} \dots \bar{g}_{ar1} \bar{g}_{ar2} \dots \alpha_{ar1} \alpha_{ar2} \dots\}^T$$

$$[\bar{E}_{s,r}] = e^{i\beta_r s} [1] \quad (2)$$

An interblade phase angle  $\beta_r$  in the range  $0-180^\circ$  represents a forward traveling wave - a wave traveling in the direction of rotation.

In Eq. (2) the standard nonrotating orthonormal modes for a beam with fixed-free boundary conditions are given by

$$W_j(\bar{n}) = \cosh(p_j \bar{n}) - \cos(p_j \bar{n}) - \frac{(\cos p_j + \cosh p_j)}{(\sin p_j + \sinh p_j)} [\sin(p_j \bar{n}) - \sin(p_j \bar{n})] \quad (3)$$

$$A_j(\bar{n}) = \sqrt{2} \sin[(2j - 1) \pi/2 \bar{n}]$$

where the value of  $p_j$  is obtained from

$$\cos p_j \cosh p_j + 1 = 0 \quad (4)$$

In the case of a tuned cascade it is adequate to analyze the motion of a cascade in each of the interblade phase angle modes separately. Hence, the total number of degrees of freedom of a tuned cascade is  $(M_h + M_g + M_\alpha)$  for each value of  $\beta_r$ .

### C. Mistuned Cascade Model

In the case of an arbitrarily mistuned cascade, the blades can have different amplitudes, and the phase angle between adjacent blades can vary. However, the general motion of a blade in a mistuned cascade can be expressed as a linear combination of the motions in all possible interblade phase angle modes of the corresponding tuned cascade. Consequently, the blade deflections can be written as

$$\begin{Bmatrix} w/b_R \\ u/b_R \\ \alpha \end{Bmatrix} = [\bar{W}]\{X_s\} e^{i \frac{\omega}{\omega_0} \tau} \\ = \sum_{r=0}^{N-1} [\bar{E}_{s,r}][\bar{W}]\{Y_r\} e^{i \frac{\omega}{\omega_0} \tau} \quad (5)$$

For a case with  $N$  mistuned blades, Eq. (5) can be generalized as

$$[W]\{X\} e^{i \frac{\omega}{\omega_0} \tau} = [E][W]\{Y\} e^{i \frac{\omega}{\omega_0} \tau} \quad (6)$$

where

$$[W] = \begin{bmatrix} [W] & & & \\ & [W] & & \\ & & \ddots & \\ & & & [W] \end{bmatrix} \\ \{X\} = \begin{Bmatrix} \{X_0\} \\ \{X_1\} \\ \vdots \\ \{X_{N-1}\} \end{Bmatrix} \quad \{Y\} = \begin{Bmatrix} \{Y_0\} \\ \{Y_1\} \\ \vdots \\ \{Y_{N-1}\} \end{Bmatrix} \\ [E] = \begin{bmatrix} [E_{0,0}] & [E_{0,1}] & \dots & \\ [E_{1,0}] & [E_{1,1}] & \dots & \\ \vdots & \vdots & & \\ & & & [E_{N-1,N-1}] \end{bmatrix} \quad (7)$$

The total number of degrees of freedom for this general case is  $N$  times  $(M_h + M_g + M_\alpha)$ .

#### D. Aerodynamic Model

The unsteady, two-dimensional, cascade, aerodynamic loads were calculated by using Smith's theory in subsonic flow, and Adamczyk and Goldstein's<sup>12</sup> theory in supersonic flow with a subsonic leading edge. In these theories, the airfoil thickness, camber and steady state angle of attack are neglected, and the flow is assumed to be isentropic and irrotational. At any radial station the relative Mach number is a function of the inflow conditions and the rotor speed. Most current fan designs have supersonic flow at the tip and subsonic flow at the root. As a result, some region of the blade span encounters transonic flow. Since the above unsteady theories are not valid in the transonic region, the subsonic theory with  $M_{eff} = 0.9$  for stations in the range  $0.9 \leq M_{eff} < 1$  and the supersonic theory with  $M_{eff} = 1.1$  for stations in the range  $1.0 \leq M_{eff} < 1.1$  were used. The motion-dependent aerodynamic lift and moment were expressed in Ref. 1 in terms of

nondimensional coefficients. The expressions for lift and moment per unit span as a function of the same coefficients can be written as

$$L_a = -\pi \rho_a b_R^3 \omega^2 \sum_{r=0}^{N-1} \left[ l_{hhr} \left( \frac{b}{b_R} \right)^2 \right. \\ \left. \cdot \left[ \cos \xi \sum_{j=1}^{M_h} W_j(\bar{n}) \bar{h}_{arj} + \sin \xi \sum_{j=1}^{M_g} W_j(\bar{n}) \bar{g}_{arj} \right] \right. \\ \left. + l_{har} \left( \frac{b}{b_R} \right)^3 \sum_{j=1}^{M_\alpha} A_j(\bar{n}) \alpha_{arj} \right] e^{i \left( \frac{\omega}{\omega_0} \tau + \beta_r s \right)} \quad (8a)$$

$$M_a = \pi \rho_a b_R^4 \omega^3 \sum_{r=0}^{N-1} \left[ l_{ahr} \left( \frac{b}{b_R} \right)^3 \right. \\ \left. \cdot \left[ \cos \xi \sum_{j=1}^{M_h} W_j(\bar{n}) \bar{h}_{arj} + \sin \xi \sum_{j=1}^{M_g} W_j(\bar{n}) \bar{g}_{arj} \right] \right. \\ \left. + l_{aar} \left( \frac{b}{b_R} \right)^4 \sum_{j=1}^{M_\alpha} A_j(\bar{n}) \alpha_{arj} \right] e^{i \left( \frac{\omega}{\omega_0} \tau + \beta_r s \right)} \quad (8b)$$

The coefficients  $l_{hhr}$ ,  $l_{har}$ , ...,  $l_{aar}$  are calculated for specified values of  $M_{eff}$ ,  $k$ ,  $s/c$ ,  $\xi$ , and  $a$ . In the aerodynamic theories used herein, the steady state angle of attack is neglected. In applying these theories to the present case, the blade steady state angle of attack is also set to zero and the effective relative velocity is assumed to be the component of the blade relative velocity along the blade chord as indicated in Fig. 2.

#### E. Structural Model

The structural model of each blade consists of a straight, slender, twisted, nonuniform elastic beam with a symmetric cross section. The elastic axis, the inertia axis, and the tension axis are taken to be noncoincident. The effect of warping is not explicitly considered. However, a partial effect of warping enters into the equations of motion as it does in Ref. 4. The blade is assumed to be rigid in the direction along the elastic axis. Consequently, the axial equation of motion is eliminated. The structural model has its basis

in the geometric nonlinear theory of elasticity in which elongations and shears are negligible compared to unity and the squares of the derivatives of the extensional deformation of the elastic axis are negligible compared to the squares of the bending slopes. This level of the geometric nonlinear theory of elasticity is required to derive a set of linear coupled bending-torsion equations of motion.

#### F. Equations of Motion

The equations of motion will be derived by using the extended Hamilton's principle in the form

$$\int_{t_0}^{t_1} (\delta T_k - \delta U + \delta W) dt = 0 \quad (9)$$

The expressions for strain energy, kinetic energy, and virtual work of aerodynamic forces can be written as

$$U = \frac{1}{2} \int_{R_H}^{R_T} \iint_A [E\gamma_{yy}^2 + G(\gamma_{yz}^2 + \gamma_{yx}^2)] dr dx dz \quad (10)$$

$$T_k = \frac{1}{2} \int_{R_H}^{R_T} \iint_A \rho_m \frac{d\bar{r}_1}{dt} \cdot \frac{d\bar{r}_1}{dt} dr dx dz \quad (11)$$

$$\delta W = \int_{R_H}^{R_T} (-L_a \sin \xi \delta u - L_a \cos \xi \delta w + M_a \delta \alpha) dr \quad (12)$$

where

$$\frac{d\bar{r}_1}{dt} = \frac{\partial \bar{r}_1}{\partial t} + \bar{\omega} \times \bar{r}_1$$

$$\bar{\omega} = \Omega(\bar{e}_x \cos \xi + \bar{e}_z \sin \xi)$$

$$\begin{aligned} \bar{r}_1 = & (r - U_F)\bar{e}_y + (u \cos \xi - w \sin \xi)\bar{e}_x \\ & + (u \sin \xi + w \cos \xi)\bar{e}_z + [T]^T \begin{Bmatrix} x \\ r \\ z \end{Bmatrix} \end{aligned} \quad (13)$$

The expressions for the strain components, position vector, foreshortening, and transformation matrix are developed in Appendix A. Substituting Eqs. (A9b), (A9c), and (A14) into Eq. (10), Eq. (13) into Eq. (11), Eqs. (8a) and (8b) into Eq. (12), the resulting equations into Eq. (9), taking the indicated variations, integrating over the cross section of the blade wherever necessary, integrating by parts over time, neglecting Coriolis and rotary inertia terms, and retaining only first-degree terms in  $u$ ,  $w$ , and  $\alpha$  yields

$$\begin{aligned} & \left[ (EI_{zz} \sin^2 \xi + EI_{xx} \cos^2 \xi) w'' \right. \\ & - (EI_{zz} - EI_{xx}) u'' \sin \xi \cos \xi - EB_2 \xi' \alpha' \sin \xi \\ & \left. - T_c e_A \alpha \cos \xi \right]'' - (T_c w')' + m\ddot{w} + m e \ddot{\alpha} \cos \xi \\ & - \Omega^2 [(m r e \alpha \cos \xi)'] + m\dot{w} + m e \alpha \cos \xi = -L_a \cos \xi \end{aligned} \quad (14a)$$

$$\begin{aligned} & \left[ (EI_{zz} \cos^2 \xi + EI_{xx} \sin^2 \xi) u'' \right. \\ & - (EI_{zz} - EI_{xx}) w'' \sin \xi \cos \xi - EB_2 \xi' \alpha' \cos \xi \\ & \left. - T_c e_A \alpha \sin \xi \right]'' - (T_c u')' + m\ddot{u} + m e \ddot{\alpha} \sin \xi \\ & - \Omega^2 (m r e \alpha \sin \xi)' = -L_a \sin \xi \end{aligned} \quad (14b)$$

$$\begin{aligned} & - [GJ \alpha' + EB_1 \xi'^2 \alpha' + T_c k_A^2 \alpha' \\ & + EB_2 \xi' (u'' \cos \xi - w'' \sin \xi)]' - T_c e_A w'' \cos \xi \\ & - T_c e_A u'' \sin \xi + m (k_m^2 \ddot{\alpha} + e \ddot{u} \sin \xi + e \ddot{w} \cos \xi) \\ & + m \Omega^2 r e (w' \cos \xi + u' \sin \xi) - m \dot{\Omega}^2 \\ & \cdot \left[ (k_{m2}^2 - k_{m1}^2) \alpha \cos 2\xi + w e \cos \xi \right] = M_a \end{aligned} \quad (14c)$$

The sectional properties in these equations are defined in Appendix B.

By substituting Eqs. (8a) and (8b) into Eqs. (14a), (14b), and (14c), nondimensionalizing the resulting equations, applying Galerkin's method, and extending the resultant equations to all the blades by using Eq. (6), the equations of motion of an arbitrarily mistuned cascade can be simplified as

$$[P]\{Y\} = \gamma[Q]\{Y\} \quad (15)$$

where

$$[Q] = [E]^{-1}[M][E] + [A]$$

$$[P] = [E]^{-1}[S][E]$$

$$\gamma = (\omega/\omega_0)^2$$

$$\begin{aligned}
 [M] &= \begin{bmatrix} [M_0] & & & \\ & [M_1] & & \\ & & \ddots & \\ & & & [M_{N-1}] \end{bmatrix} \\
 [A] &= \begin{bmatrix} [A_0] & & & \\ & [A_1] & & \\ & & \ddots & \\ & & & [A_{N-1}] \end{bmatrix} \\
 [S] &= \begin{bmatrix} [S_0] & & & \\ & [S_1] & & \\ & & \ddots & \\ & & & [S_{N-1}] \end{bmatrix}
 \end{aligned} \tag{16}$$

As indicated in Eq. (B2), structural damping is added by multiplying the direct stiffness coefficients by  $(1 + 2i\zeta_{hs1})$ ,  $(1 + 2i\zeta_{hs2})$ , ...  $(1 + 2i\zeta_{as2})$  ...

### III. Results and Discussion

#### A. Solution

The aeroelastic stability boundaries are obtained by solving the standard complex eigenvalue problem represented by Eq. (15). The relation between the frequency  $\omega$  and  $\gamma$  is

$$i \frac{\omega}{\omega_0} = i\sqrt{\gamma} = \bar{\mu} \pm i\bar{\nu} \tag{17}$$

Flutter occurs when  $\bar{\mu} > 0$ .

#### B. Computer Program and Verification

A computer program (ASTROMIC) was written to assemble and solve the generalized eigenvalue problem given in Eq. (15). The program can be used to predict the in vacuum natural frequencies of a nonuniform rotating beam by setting the aerodynamic matrix  $[A]$  to zero. In this case the problem is reduced to a standard eigensolution. For the flutter problem, the aerodynamic matrix is a function of the eigenvalues. Hence, an iterative solution is required. The iterative technique used herein to calculate flutter boundaries (once the problem is completely described) is briefly summarized as follows:

1. Select an axial Mach number.
2. Select a rotation speed and assemble the stiffness and mass matrices.
3. Calculate the variation of the reduced frequency based on an assumed reference frequency  $\omega_0$  and relative Mach number with span and construct the aerodynamic matrix. The initial value for the reference frequency is the same as the natural frequency of the mode of interest.
4. Solve the eigenvalue problem.

5. For the mode of interest check whether the imaginary part of the eigenvalue is within an acceptable tolerance of the reference frequency. If not, go back to step (3) with a new reference frequency.
6. For the mode of interest, check whether the real part of the eigenvalue is within an acceptable tolerance of unity. If not, modify the rotational speed and repeat the process from step (2). If positive, reduce speed; if negative, increase speed.
7. To find the flutter boundary for another value of the axial Mach number go back to step (1).

It should be noted that the above method utilizes a rotor speed iteration within the axial Mach number iteration loop. It would appear that it would be more efficient to place the Mach number iteration within the rotor speed iteration loop, since the mass and stiffness matrices have to be updated each time the rotor speed is changed. However, it was found that the time required to assemble these matrices is small relative to the time required to assemble the aerodynamic matrix and to extract the eigenvalues and eigenvectors. In addition, the flutter boundary was more "distinct" using the method described above.

The correctness of the program was checked by constructing a hypothetical blade model with constant structural and aerodynamic properties along the span. The blade frequencies obtained by using the program were checked against known solutions. The eigensolutions with aerodynamics included were checked against the results obtained by using the typical section model program (MISER) developed in Refs. 1 and 2.

For a cascade with nonuniform blades, there are no published theoretical results on flutter. However the results from ASTROMIC are compared with those from MISER by choosing the properties for a typical section at different spanwise stations. These results will be discussed later.

#### C. Aeroelastic Stability of an Advanced Fan

An advanced unshrouded fan stage (aspect ratio = 3.3), representative of a next generation fan, was chosen for analysis. A similar stage was analyzed in Ref. 3 by using the typical section model. The results in Ref. 3 indicated that the fan design without shrouds did not meet the flutter requirements, but that it may be feasible to use mistuning as a passive flutter control. The motivation for choosing this fan stage for analysis herein is to further investigate the use of mistuning as a passive flutter control.

The properties of the fan blade are listed in Table I and the reference properties are listed in Table II. The design point is at a rotor speed of 4267 rev/min. and an axial Mach number of 0.55. At these conditions the tip relative Mach number is 1.45.

The analyses are performed using two modes each in the plane of rotation, in the plane perpendicular to the plane of rotation, and in torsion. Since there are 28 blades in this stage and hence 28 interblade phase angle modes, the total number of degrees of freedom for an arbitrarily mistuned cascade is 168. However, for alternate



mistuning, in which every other blade is identical, certain symmetry properties are exploited in the analysis. Because of symmetry, the  $\beta_r$  mode couples with the  $(\beta_r + \pi)$  mode only. The analysis for this case consists of 14 separate eigensolutions of 12 degrees of freedom each rather than one eigensolution of 168 degrees of freedom for an arbitrarily mistuned cascade.

The blade was analyzed for vibration to generate a Campbell diagram which is shown in Fig. 3. Only the first and second bending frequencies and the first torsion frequency are shown. Since the mass ratio for this blade is high, the aerodynamic forces result in flutter frequencies which are not significantly different from those in a vacuum.

In Refs. 1-3, a typical section model, which was originally used for fixed wing flutter analysis, was adapted for rotating blades. In the case of a fixed wing, the relative velocity of each strip along the span is constant; the structural properties of the typical section are obtained by their respective values at the 3/4 blade span station. In the case of a rotating blade, the relative velocity of each strip along the blade varies. Then, a question arises as to which spanwise station should be used as a reference to calculate the structural and aerodynamic properties of the typical section. To answer this question, the eigenvalues of the tuned cascade at the design condition from both the present beam and typical section analyses using various spanwise locations as reference are compared in Fig. 4. As expected, the cascade is unstable over a range of interblade phase angles corresponding to forward traveling waves. It should be noted that, whereas there are 168 eigenvalues, only the predominantly torsional eigenvalues are shown. The other modes were found to be stable at the design condition. Also, it can be seen that the typical section model corresponding to approximately the 7/10 span reference station gives the best correlation for the unstable modes with the nonuniform blade model. This finding is in close agreement with the 3/4 span reference station usually used for fixed wing aeroelastic calculations. This observation is very useful in performing preliminary aeroelastic analyses.

Previous publications<sup>1-3</sup> using the typical section model have shown that torsional frequency mistuning could have a significant stabilizing effect on the cascade. The effect of mistuning is further investigated herein with the nonuniform blade model. The method used to vary the frequency from blade-to-blade was simply to vary the torsional stiffness,  $J$ . For alternate mistuning, the torsional stiffness of the odd numbered blades was increased by 10 percent over that of a tuned blade at each spanwise location. Likewise, the torsional stiffnesses of the even numbered blades was decreased by 10 percent from that of a tuned blade. The result was a total torsional frequency variation of approximately 7 percent. The eigenvalues for this mistuned rotor at the design conditions are shown in Fig. 5, along with the corresponding tuned values. These predominately torsional eigenvalues have split into high and low frequency families corresponding to modes with major participation of the odd and even blades, respectively. As can be seen, this type of mistuning has stabilized the cascade to such an extent that it is stable at the design point.

By using the iterative procedure defined above the flutter boundaries for both the tuned and mistuned cascades were calculated. The results are shown in Fig. 6. For the tuned cascade it is seen that the design point lies well inside in the unstable region. As expected, the axial Mach number at flutter monotonically decreases with increasing rotor speed. For the tuned cascade it should also be noted that along the flutter boundary the tip relative Mach number is approximately 1.15. Consequently, a region near the blade tip may experience nonlinearities associated with transonic flow which are not accounted for by the unsteady aerodynamic theories used herein. The relative tip Mach number at the design conditions is 1.45.

The inclusion of an alternate frequency mistuning of approximately 7 percent has significantly increased the cascade stability by moving the flutter boundary to the right. Furthermore, the design point is stable for this level of mistuning. The mode defining the boundary has maximum participation of the even-numbered (or low frequency) blades. The tip relative Mach number along the boundary of the mistuned cascade is 1.53. Consequently, the transonic region is considerably inboard of the tip and the transonic effects should be minimal.

Figure 6 also illustrates the effect of structural damping on flutter of a tuned cascade. A structural damping ratio of 0.002 is included in each of the torsional modes. As can be seen, the damping has a significantly stabilizing effect on flutter speed of a tuned cascade.

#### IV. Conclusions

The major conclusions from this investigation are summarized as follows:

1. A general expression for foreshortening of a blade was derived and was explicitly used in deriving the first-degree linear equations of motion of a rotating blade.
2. An aeroelastic model and an associated computer program for a mistuned cascade with nonuniform blades were developed.
3. For the blade analyzed herein a typical section model corresponding to the 7/10 span reference station gives the best correlation with the nonuniform blade model.
4. An advanced, unshrouded, high-aspect ratio fan was modelled and analyzed with and without mistuning. The results show that a moderate amount of mistuning has enough potential to alleviate flutter problems in unshrouded turbofans.

#### Appendix A

##### Strain Displacement Relations

A schematic representation of the deformed and undeformed elastic axis is shown in Fig. 1. Since the pretwist angle  $\xi$  varies with  $r$ , with initial curvature of the elastic axis is

$$\bar{\omega}_{xyz} = \bar{e}_y \frac{d\xi}{dr} = \bar{e}_y \xi' \quad (A1)$$

The elastic deformations translate and rotate the triad  $xyz$  to  $x_3y_3z_3$ . Let the expressions for the curvature vector of the deformed elastic axis and for the transformation matrix between the  $x_3y_3z_3$  and  $xyz$  systems be

$$\bar{w}_{x_3y_3z_3} = \omega_{x_3}\bar{e}_{x_3} + \omega_{y_3}\bar{e}_{y_3} + \omega_{z_3}\bar{e}_{z_3} \quad (A2)$$

$$\begin{Bmatrix} \bar{e}_{x_3} \\ \bar{e}_{y_3} \\ \bar{e}_{z_3} \end{Bmatrix} = [T] \begin{Bmatrix} \bar{e}_x \\ \bar{e}_y \\ \bar{e}_z \end{Bmatrix} \quad (A3)$$

Following the procedure presented in Ref. 8, one can develop the second-degree expressions for the curvature components and for the transformation matrix in terms of  $u$ ,  $v$ ,  $w$ , and  $\alpha$  as

$$\omega_{x_3} = (u'' + \alpha w'') \sin \xi + (w'' - \alpha u'') \cos \xi$$

$$\omega_{y_3} = -\alpha' + \xi' \left( 1 - \frac{u'^2}{2} - \frac{w'^2}{2} \right) + (u' \sin \xi + w' \cos \xi)' (u' \cos \xi - w' \sin \xi)$$

$$\omega_{z_3} = -(u'' + \alpha w'') \cos \xi + (w'' - \alpha u'') \sin \xi \quad (A4)$$

$$[T] = \begin{bmatrix} 1 - \frac{1}{2}(u' \cos \xi - w' \sin \xi)^2 - \frac{\alpha^2}{2} & u' \cos \xi - w' \sin \xi & -\alpha \\ -\frac{1}{2}(u' \cos \xi - w' \sin \xi) & 1 - \frac{u'^2}{2} - \frac{w'^2}{2} & \alpha(u' \cos \xi - w' \sin \xi) \\ -\alpha(u' \sin \xi + w' \cos \xi) & u' \sin \xi + w' \cos \xi & -(u' \sin \xi + w' \cos \xi) \\ \alpha - \frac{1}{2}(u' \cos \xi - w' \sin \xi) & u' \sin \xi + w' \cos \xi & 1 - \frac{\alpha^2}{2} - \frac{1}{2}(u' \sin \xi + w' \cos \xi)^2 \end{bmatrix} \quad (A5)$$

From Fig. 1, the position vector of an arbitrary point on the blade before deformation is

$$\bar{r}_0 = \bar{R}_0(r) + x\bar{e}_x + z\bar{e}_z \quad (A6)$$

and that of the same point after deformation is

$$\bar{r}_1 = \bar{R}_1(r_1) + x\bar{e}_{x_3} + z\bar{e}_{z_3} \quad (A7)$$

Then, the Green's strain tensor based on a Lagrangian description is given by

$$d\bar{r}_1 \cdot d\bar{r}_1 - d\bar{r}_0 \cdot d\bar{r}_0 = 2 \left[ dx \ dr \ dz \right] [\epsilon_{ij}] \begin{Bmatrix} dx \\ dr \\ dz \end{Bmatrix} \quad (A8)$$

Substituting Eqs. (A6) and (A7) into Eq. (A8) and retaining terms up to second-degree in  $u$ ,  $v$ ,  $w$ , and  $\alpha$ , one obtains the following expressions for the required components of strain:

$$\begin{aligned} \epsilon_{yy} &= v' + \frac{1}{2}(u'^2 + w'^2) \\ &\quad - z[(u'' + \alpha w'') \sin \xi + (w'' - \alpha u'') \cos \xi] \\ &\quad - x[(u'' + \alpha w'') \cos \xi - (w'' - \alpha u'') \sin \xi] \\ &\quad + \frac{z^2 + x^2}{2}(\alpha'^2 - 2\alpha'\xi') \end{aligned} \quad (A9a)$$

$$\begin{aligned} \epsilon_{yx} &= \frac{z}{2} \left[ -\alpha' - \frac{\xi'}{2}(u'^2 + w'^2) \right. \\ &\quad \left. + (u' \sin \xi + w' \cos \xi)' \cdot (u' \cos \xi - w' \sin \xi) \right] \end{aligned} \quad (A9b)$$

$$\begin{aligned} \epsilon_{yz} &= -\frac{x}{2} \left[ -\alpha' - \frac{\xi'}{2}(u'^2 + w'^2) \right. \\ &\quad \left. + (u' \sin \xi + w' \cos \xi)' \cdot (u' \cos \xi - w' \sin \xi) \right] \end{aligned} \quad (A9c)$$

Invoking the small strain assumption, the engineering strains are related to the components of the strain tensor according to:

$$\gamma_{yy} = \epsilon_{yy}; \quad \gamma_{yx} = 2\epsilon_{yx}; \quad \gamma_{yz} = 2\epsilon_{yz} \quad (A10)$$

It should be pointed out that in arriving at the expressions given in Eq. (A9) several higher-order terms have been discarded based either on considerations related to small deformations or on approximations due to slenderness of the blade.

It is convenient to eliminate the axial equation of motion. This is done by explicitly considering the foreshortening due to bending and torsion. The expression for foreshortening for the present case is derived by making use of the equilibrium condition that the integral of the longitudinal stress over the cross section must be equal to the total tension. Thus,

$$\begin{aligned} T_C &= E \iint_A \gamma_{yy} \, dx \, dz \\ &= EA \left[ v' + \frac{1}{2}(u'^2 + w'^2) - e_A [(u'' + \alpha w'') \cos \xi \right. \\ &\quad \left. - (w'' - \alpha u'') \sin \xi] + k_A^2 \left( \frac{\alpha'^2}{2} - \alpha'\xi' \right) \right] \end{aligned} \quad (A11)$$

from which

$$v' = v_e' - U_F' \quad (A12)$$

where

$$v_e' = \frac{T_C}{EA}$$

$$U_F = \int_{R_H}^r \left\{ \frac{1}{2} (u'^2 + w'^2) - e_A [(u'' + \alpha w'') \cos \xi - (w'' - \alpha u'') \sin \xi] + k_A^2 \left( \frac{\alpha'^2}{2} - \alpha' \xi' \right) \right\} dr \quad (A13)$$

An alternate expression for  $T_C$  results from the kinetic energy and is given in Appendix B. Substituting Eqs. (A12) and (A13) into Eq. (A9a) and invoking the assumption that the blade is rigid ( $EA \rightarrow \infty$ ) along its elastic axis, one obtains

$$\begin{aligned} \gamma_{yy} = & -z[(u'' + \alpha w'') \sin \xi + (w'' - \alpha u'') \cos \xi] \\ & - (x - e_A)[(u'' + \alpha w'') \cos \xi - (w'' - \alpha u'') \sin \xi] \\ & + \frac{1}{2} (z^2 + x^2 - k_A^2) (\alpha'^2 - 2\alpha' \xi') \end{aligned} \quad (A14)$$

The other components of strain given by Eqs. (A9b) and (A9c) remain unchanged.

#### Appendix B

##### Sectional Properties and Definition of Matrices

$$T_C = \int_r^{R_T} m \omega^2 r \, dr$$

$$I_{xx} = \iint z^2 \, dx \, dz$$

$$I_{zz} = \iint x^2 \, dx \, dz - e_A^2 A$$

$$B_1 = \iint (x^2 + z^2 - k_A^2)^2 \, dx \, dz$$

$$B_2 = \iint (x - e_A) (x^2 + z^2 - k_A^2) \, dx \, dz$$

$$J = \iint (x^2 + z^2) \, dx \, dz$$

$$A = \iint dx \, dz$$

$$Ae_A = \iint x \, dx \, dz$$

$$Ak_A^2 = \iint (x^2 + z^2) \, dx \, dz$$

$$m = \iint \rho_m \, dx \, dz$$

$$me = \iint \rho_m x \, dx \, dz$$

$$mk_{m1}^2 = \iint \rho_m z^2 \, dx \, dz$$

$$mk_{m2}^2 = \iint \rho_m x^2 \, dx \, dz$$

$$k_m^2 = k_{m1}^2 + k_{m2}^2$$

(B1)

Note the expression for  $J$  is valid only for a circular section. For a noncircular section a warping correction must be included.

$$[M_s] = \begin{bmatrix} M_{hhs11} & M_{hhs12} & \cdots & M_{hgs11} & M_{hgs12} & \cdots & M_{has11} & M_{has12} & \cdots \\ M_{hhs21} & M_{hhs22} & \cdots & M_{hgs21} & M_{hgs22} & \cdots & M_{has21} & M_{has22} & \cdots \\ \vdots & \vdots & & & & & & & \\ M_{ghs11} & M_{ghs12} & \cdots & M_{ggs11} & M_{ggs12} & \cdots & M_{gas11} & M_{gas12} & \cdots \\ M_{ghs21} & M_{ghs22} & \cdots & M_{ggs21} & M_{ggs22} & \cdots & M_{gas21} & M_{gas22} & \cdots \\ \vdots & \vdots & & & & & & & \\ M_{ahs11} & M_{ahs12} & \cdots & M_{ags11} & M_{ags12} & \cdots & M_{aas11} & M_{aas12} & \cdots \\ M_{ahs21} & M_{ahs22} & \cdots & M_{ags21} & M_{ags22} & \cdots & M_{aas21} & M_{aas22} & \cdots \\ \vdots & \vdots & & & & & & & \end{bmatrix}$$

$$[S_s] = \begin{bmatrix} S_{hhs11}(1 + 2i\zeta_{hs1}) & S_{hhs12} & \cdots & S_{hgs11} & S_{hgs12} & \cdots & S_{has11} & S_{has12} & \cdots \\ S_{hhs21} & S_{hhs22}(1 + 2i\zeta_{hs2}) & \cdots & & & & & & \\ \vdots & \vdots & & & & & & & \\ & & & & & & S_{\alpha as21} & S_{\alpha as22}(1 + 2i\zeta_{\alpha s2}) & \cdots \\ \vdots & \vdots & & & & & & & \end{bmatrix} \quad (B2)$$

$$[A_r] = \begin{bmatrix} L_{hhr11} & L_{hhr12} & \cdots & L_{hgr11} & L_{hgr12} & \cdots & L_{har11} & L_{har12} & \cdots \\ L_{hhr21} & L_{hhr22} & \cdots & L_{hgr21} & L_{hgr22} & \cdots & L_{har21} & L_{har22} & \cdots \\ \vdots & \vdots & & & & & & & \\ L_{ghr11} & L_{ghr12} & \cdots & L_{ggr11} & L_{ggr12} & \cdots & L_{gar11} & L_{gar12} & \cdots \\ L_{ghr21} & L_{ghr22} & \cdots & L_{ggr21} & L_{ggr22} & \cdots & L_{gar21} & L_{gar22} & \cdots \\ \vdots & \vdots & & & & & & & \\ L_{ahr11} & L_{ahr12} & \cdots & L_{agr11} & L_{agr12} & \cdots & L_{aar11} & L_{aar12} & \cdots \\ L_{ahr21} & L_{ahr22} & \cdots & L_{agr21} & L_{agr22} & \cdots & L_{aar21} & L_{aar22} & \cdots \\ \vdots & \vdots & & & & & & & \end{bmatrix} \quad (B3)$$

$$S_{hhsij} = \frac{EI_{xx0}}{m_0 L^4 \omega_0^2} S_{1sij} + \left(\frac{\Omega}{\omega_0}\right)^2 [S_{7sij} - S_{3sij}]$$

$$S_{hgsij} = -\frac{EI_{xx0}}{m_0 L^4 \omega_0^2} S_{2sij}$$

$$S_{h\alpha ij} = \left(\frac{\Omega}{\omega_0}\right)^2 [S_{8sij} - S_{10sij} - S_{21sij}] - \frac{GJ_0}{m_0 \omega_0^2 L^3 b_R} S_{20sij}$$

$$S_{ggsij} = \frac{EI_{xx0}}{m_0 L^4 \omega_0^2} S_{25sij} + \left(\frac{\Omega}{\omega_0}\right)^2 S_{7sij}$$

$$S_{ghsij} = -\frac{EI_{xx0}}{m_0 L^4 \omega_0^2} S_{2sij}$$

$$S_{g\alpha sij} = \left(\frac{\Omega}{\omega_0}\right)^2 (S_{32sij} - S_{44sij}) + \frac{GJ_0}{m_0 L^3 b_R \omega_0^2} S_{43sij}$$

$$S_{ahsij} = -\frac{GJ_0 S_{71sij}}{m_0 \omega_0^2 L^3 b_R r_{\alpha_0}^2} - \left(\frac{\Omega}{\omega_0}\right)^2 \cdot (-S_{58sij} + S_{54sij} + S_{72sij}) \frac{1}{r_{\alpha_0}^2}$$

$$S_{agsij} = -\frac{GJ_0 S_{70sij}}{m_0 \omega_0^2 L^3 b_R r_{\alpha_0}^2} - \left(\frac{\Omega}{\omega_0}\right)^2 \frac{1}{r_{\alpha_0}^2} (S_{73sij} - S_{59sij})$$

$$S_{\alpha\alpha sij} = \frac{GJ_0}{m_0 k m_0 L^2 \omega_0^2} (S_{51sij} + S_{69sij}) + \left(\frac{\Omega}{\omega_0}\right)^2 \left( \frac{S_{57sij}}{r_{\alpha_0}^2} - S_{60sij} \right) \quad (B4)$$

$$L_{hhrij} = \frac{1}{\nu_0} \int_0^1 \left(\frac{b}{b_R}\right)^2 l_{hhr} W_i W_j \cos^2 \xi \, d\bar{n}$$

$$L_{hgrij} = \frac{1}{\nu_0} \int_0^1 \left(\frac{b}{b_R}\right)^2 l_{hhr} W_j W_i \sin \xi \cos \xi \, d\bar{n}$$

$$L_{harij} = \frac{1}{\nu_0} \int_0^1 \left(\frac{b}{b_R}\right)^3 l_{har} A_j W_i \cos \xi \, d\bar{n}$$

$$L_{ghrij} = \frac{1}{\nu_0} \int_0^1 \left(\frac{b}{b_R}\right)^2 l_{hhr} W_j W_i \sin \xi \cos \xi \, d\bar{n}$$

$$L_{ggrij} = \frac{1}{\nu_0} \int_0^1 \left(\frac{b}{b_R}\right)^2 l_{hhr} W_j W_i \sin^2 \xi \, d\bar{n}$$

$$L_{garij} = \frac{1}{\nu_0} \int_0^1 \left(\frac{b}{b_R}\right)^3 l_{har} A_j W_i \sin \xi \, d\bar{n}$$

$$L_{ahrj} = \frac{1}{\nu_0 r_{\alpha_0}^2} \int_0^1 \left(\frac{b}{b_R}\right)^3 l_{ahr} W_j A_i \cos \xi \, d\bar{n}$$

$$L_{agrj} = \frac{1}{\nu_0 r_{\alpha_0}^2} \int_0^1 \left(\frac{b}{b_R}\right)^3 l_{ahr} W_j A_i \sin \xi \, d\bar{n}$$

$$L_{\alpha\alpha rij} = \frac{1}{\nu_0 r_{\alpha_0}^2} \int_0^1 \left(\frac{b}{b_R}\right)^4 l_{\alpha\alpha r} A_j A_i \, d\bar{n} \quad (B5)$$

$$S_{1sij} = \int_0^1 (\overline{EI}_{zz} \sin^2 \xi + \overline{EI}_{xx} \cos^2 \xi) W_j'' W_i'' \, d\bar{n}$$

$$S_{2sij} = \int_0^1 (\overline{EI}_{zz} - \overline{EI}_{xx}) W_j'' W_i'' \sin \xi \cos \xi \, d\bar{n}$$

$$S_{3sij} = M_{hhsij} = M_{ggsij} = \int_0^1 \overline{m} W_j W_i \, d\bar{n}$$

$$S_{7sij} = \int_0^1 \overline{T}_c W_j' W_i' \, d\bar{n}$$

$$S_{8sij} = \int_0^1 \overline{m} \bar{e} (\bar{e}_H + \bar{n}) A_j W_i' \cos \xi \, d\bar{n}$$

$$S_{10sij} = \int_0^1 \overline{m} \bar{e} A_j W_i \cos \xi \, d\bar{n}$$

$$S_{20sij} = \int_0^1 \overline{EB}_{2\xi} A_j' W_i'' \sin \xi \, d\bar{n}$$

$$\begin{aligned}
S_{21sij} &= \int_0^1 \bar{T}_c \bar{e}_A A_j W_i'' \sin \xi \, d\bar{n} \\
S_{25sij} &= \int_0^1 (\bar{E}I_{zz} \cos^2 \xi + \bar{E}I_{xx} \sin^2 \xi) W_j W_i'' \, d\bar{n} \\
S_{32sij} &= \int_0^1 \bar{m}(\bar{n} + \bar{e}_H) \bar{e}_A W_j' \sin \xi \, d\bar{n} \\
S_{43sij} &= \int_0^1 \bar{E}B_2 \xi' A_j W_i'' \cos \xi \, d\bar{n} \\
S_{44sij} &= \int_0^1 \bar{T}_c \bar{e}_A A_j W_i'' \sin \xi \, d\bar{n} \\
S_{51sij} &= \int_0^1 \bar{G}J A_j' A_i' \, d\bar{n} \\
S_{54sij} &= M_{ahsij} r_{\alpha_0}^2 = \int_0^1 \bar{m} \bar{e}_W W_j A_i \cos \xi \, d\bar{n} \\
S_{57sij} &= \int_0^1 \bar{T}_c \bar{k}_A^2 A_j' A_i' \, d\bar{n} \\
S_{58sij} &= \int_0^1 (\bar{n} + \bar{e}_H) \bar{e}_m W_j' A_i \cos \xi \, d\bar{n} \\
S_{59sij} &= \int_0^1 (\bar{n} + \bar{e}_H) \bar{e}_m W_j' A_i \sin \xi \, d\bar{n} \\
S_{60sij} &= \int_0^1 \bar{m} (\bar{k}_2^2 - \bar{k}_{m_1}^2) A_j A_i \cos 2\xi \, d\bar{n} \\
S_{69sij} &= \int_0^1 \bar{E}B_1 \xi'^2 A_j' A_i' \, d\bar{n} \\
S_{70sij} &= \int_0^1 \bar{E}B_2 W_j W_i' \cos \xi \, d\bar{n} \\
S_{71sij} &= \int_0^1 \bar{E}B_2 W_j W_i' \sin \xi \, d\bar{n} \\
S_{72sij} &= \int_0^1 \bar{T}_c \bar{e}_A W_j W_i' \cos \xi \, d\bar{n} \\
S_{73sij} &= \int_0^1 \bar{T}_c \bar{e}_A W_j W_i' \sin \xi \, d\bar{n} \\
M_{hasij} &= \int_0^1 \bar{m} \bar{e}_A W_j \cos \xi \, d\bar{n}
\end{aligned}$$

(B6)

$$M_{gasij} = \int_0^1 \bar{m} \bar{e}_A W_j \sin \xi \, d\bar{n}$$

$$M_{\alpha asij} = \int_0^1 \bar{m} \bar{k}_m^2 A_j A_i \, d\bar{n}$$

$$M_{agsij} r_{\alpha_0}^2 = \int_0^1 \bar{m} \bar{e}_W W_j A_i \sin \xi \, d\bar{n} \quad (B7)$$

Nondimensional Quantities

$$\bar{n} = \frac{r - R_H}{L} = \frac{n}{L}$$

$$\bar{b} = b/b_R$$

$$\bar{h}_s = h_s/b_R$$

$$\bar{g}_s = g_s/b_R$$

$$\tau = t\omega_0$$

$$\bar{E}I_{xx} = EI_{xx}/EI_{xx0}$$

$$\bar{E}I_{zz} = EI_{zz}/EI_{xx0}$$

$$\bar{G}J = GJ/GJ_0$$

$$\bar{E}A = EA/EA_0$$

$$\bar{m} = m/m_0$$

$$\bar{e}_A = e_A/b_R$$

$$\bar{e} = e/b_R$$

$$\bar{e}_H = R_H/L$$

$$\bar{T}_c = T_c/m_0 \omega^2 L^2$$

$$\bar{E}B_1 = EB_1/GJ_0 L^2$$

$$\bar{E}B_2 = EB_2/GJ_0 L$$

$$\bar{k}_m = k_m/k_{m_0}$$

$$\bar{k}_{m_1} = k_{m_1}/k_{m_0}$$

$$\bar{k}_{m_2} = k_{m_2}/k_{m_0}$$

$$r_{\alpha_0} = k_{m_0} / b_R$$

$$m_0 = A_0 \rho_m$$

$$\nu_0 = m_0 / \pi \rho_a b_R^2$$

$$\bar{k}_A = k_A / b_R$$

$$L = R_T - R_H$$

$$\frac{\partial(\quad)}{\partial t} = \frac{\partial(\quad)}{\partial \tau} \omega_0$$

$$\frac{\partial(\quad)}{\partial r} = \frac{\partial(\quad)}{L \partial \bar{n}} \quad (B7)$$

#### References

1. Kaza, Krishna Rao V. and Kielb, Robert E., "Effects of Mistuning on Bending-Torsion Flutter and Response of a Cascade in Incompressible Flow," AIAA Paper No. 81-0532 presented at the AIAA Dynamics Specialists Conference, Atlanta, Georgia, April 9-10, 1981 (DOE/NASA/1028-29; NASA TM-81674), scheduled for publication in the AIAA Journal, August or September 1982.
2. Kielb, Robert E., and Kaza, Krishna Rao V., "Aeroelastic Characteristics of a Cascade of Mistuned Blades in Subsonic and Supersonic Flows," ASME Paper No. 81-DET-122, presented at the Eighth Biennial ASME Design Engineering Conference on Mechanical Vibrations and Noise, Hartford, Connecticut, September 20-23, 1981 (NASA TM-82631), accepted for publication in the ASME Journal of Mechanical Design.
3. Kielb, Robert E., "Aeroelastic Characteristics of a Mistuned Bladed-Disc Assembly," Ph.D. Dissertation, The Ohio State University, Columbus, Ohio 1981.
4. Houbolt, J. C., and Brooks, G. W., "Differential Equations of Motion for Combined Flapwise Bending, Chordwise Bending, and Torsion of Twisted Nonuniform Rotor Blades," NACA Report 1346, 1958.
5. Hodges, D. H., and Dowell, E. H., "Nonlinear Equations of Motion for the Elastic Bending and Torsion of Twisted Nonuniform Rotor Blades," NASA TN D-2818, December 1974.
6. Rosen, A., and Friedmann, P., "Nonlinear Equations of Equilibrium for Helicopter or Wind Turbine Blades Undergoing Moderate Deformation," NASA CR-159478, December 1978.
7. Kaza, K. R. V., and Kvaternik, R. G., "Nonlinear Aeroelastic Equations for Combined Flapwise Bending, Chordwise Bending, Torsion and Extension of Twisted Nonuniform Rotor Blades in Forward Flight," NASA TM-74059, August, 1977.
8. Kaza, K. R. V., "Nonlinear Aeroelastic Equations of Motion of Twisted Nonuniform, Flexible Horizontal-Axis Wind Turbine Blades," NASA CR-159502, July 1980.
9. Kaza, K. R. V., and Kvaternik, R. G., "Aeroelastic Equations of Motion of a Darrieus Vertical-Axis Wind Turbine Blade," NASA TM-79295, December 1979.
10. Kaza, K. R. V., and Kvaternik, R. G., "Nonlinear Flap-Lag-Axial Equations of a Rotating Beam," AIAA Journal, Vol. 15, No. 6, June 1977, pp. 871-874.
11. Smith, S. N., "Discrete Frequency Sound Generation in Axial Flow Turbomachines," ARC-R&M No. 3709, 1973.
12. Adamczyk, J. J., and Goldstein, M. E., "Unsteady Flow in Supersonic Cascade with Subsonic Leading-Edge Locus," AIAA Journal, Vol. 16, No. 12, December 1978, pp. 1248-1254.
13. Lane, F., "System Mode Shapes in the Flutter of Compressor Blade Rows," Journal of the Aeronautical Sciences, Vol. 23, No. 1, Jan. 1956, pp. 54-56.

TABLE I. - BLADE SECTIONAL PROPERTIES

	$\bar{n}$							
	0.0199	0.1017	0.2372	0.4083	0.5917	0.7628	0.8983	0.9801
$\overline{EI}_{xx}$	0.9719	0.9665	0.7827	0.6072	0.3067	0.1633	0.1149	0.0839
$\overline{EI}_{zz}$	112.4	124.8	152.4	139.4	122.7	119.3	127.7	124.1
$\overline{GJ}$	0.0719	0.9665	0.7827	0.6072	0.3067	0.1633	0.1149	0.0839
$\overline{EA}$	0.9974	1.0225	0.9711	0.9358	0.7641	0.6482	0.6038	0.5541
$\overline{EB}_1$	0.4436	0.5338	0.5675	0.7275	0.6901	0.7694	0.9458	0.9734
$\overline{EB}_2$	0	0	0	0	0	0	0	0
$\overline{e}_A$	0	0	0	0	0	0	0	0
$\overline{k}_A$	0.5859	0.6095	0.6265	0.6722	0.6972	0.7461	0.7995	0.8226
$\overline{k}_{m1}$	0.0940	0.0925	0.0854	0.0767	0.0603	0.0478	0.0415	0.0370
$\overline{k}_{m2}$	1.0103	1.0516	1.0816	1.1616	1.2060	1.2913	1.3840	1.4242
$\overline{m}$	0.9974	1.0225	0.9711	0.9358	0.7641	0.6482	0.6038	0.5541
$\overline{b}$	1.010	1.051	1.082	1.161	1.206	1.291	1.384	1.425

TABLE II. - REFERENCE QUANTITIES

$N = 28$	$\rho_m = 4374 \text{ kg/m}^3$
$b_R = 0.0946 \text{ m}$	$\rho_a = 1 \text{ kg/m}^3$
$R_H = 0.3876 \text{ m}$	$a_0 = 340.3 \text{ m/sec}$
$R_T = 1.021 \text{ m}$	$A_0 = 0.0034 \text{ m}^2$
$E = 1.23 \times 10^{11} \text{ N/m}^2$	$r_{\alpha_0} = 0.5774$
$G = 4.744 \times 10^{10} \text{ N/m}^2$	$\omega_0 = \text{varies, rad/sec}$
$I_{xx0} = 9.19 \times 10^{-8} \text{ m}^4$	$M_h = M_g = M_\alpha = 2$
$J_0 = 3.676 \times 10^{-7} \text{ m}^4$	$\xi = \tan^{-1} [1.552(\bar{n} + \overline{e}_H)]$



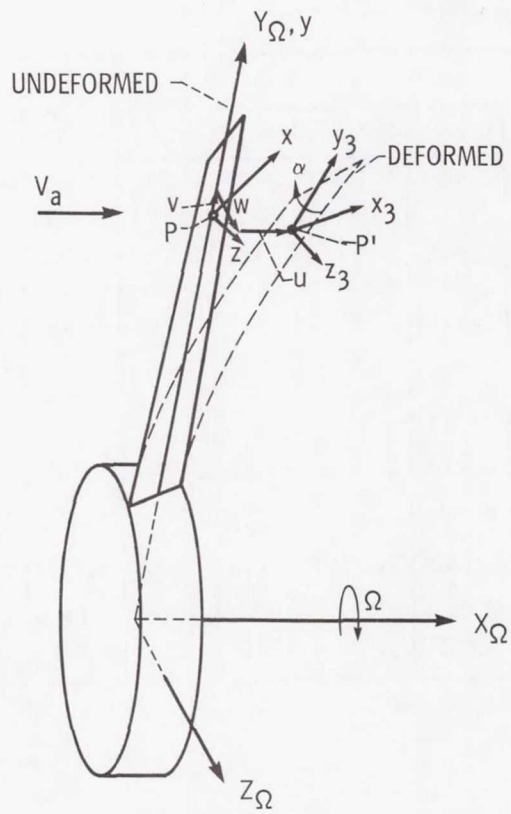


Figure 1. - Blade coordinate systems before and after deformation.

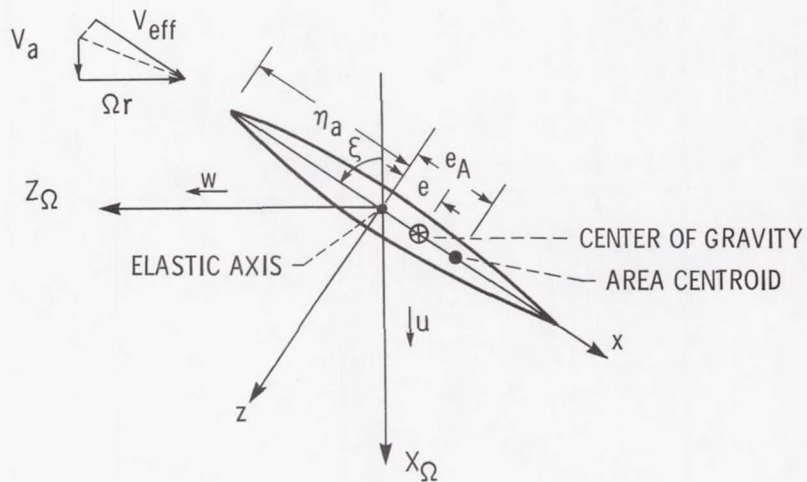


Figure 2. - Coordinate systems of blade cross section.

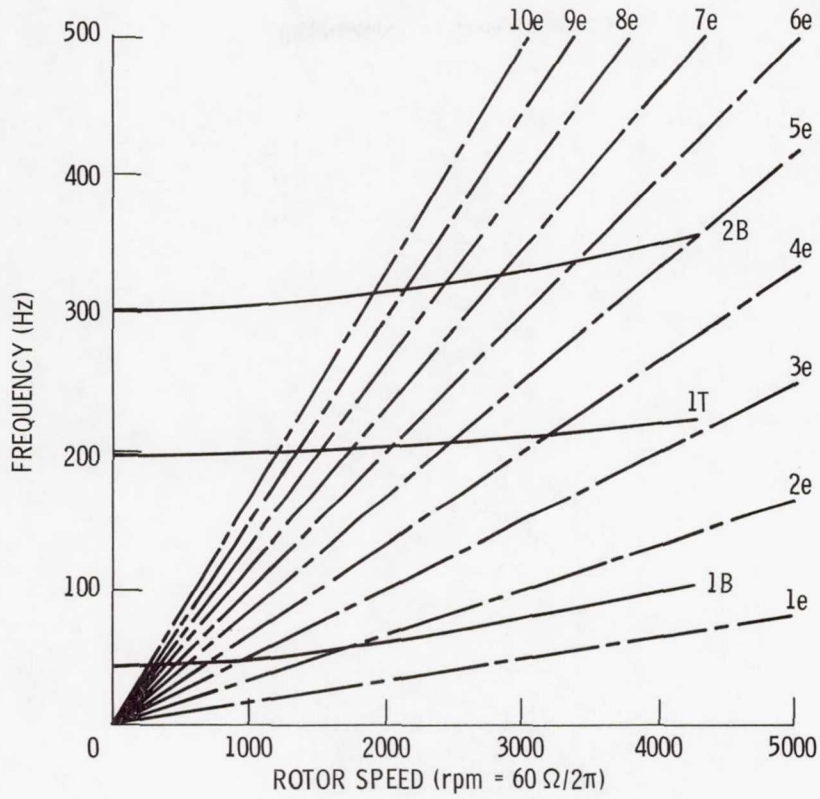


Figure 3. - Campbell diagram of the fan blade.

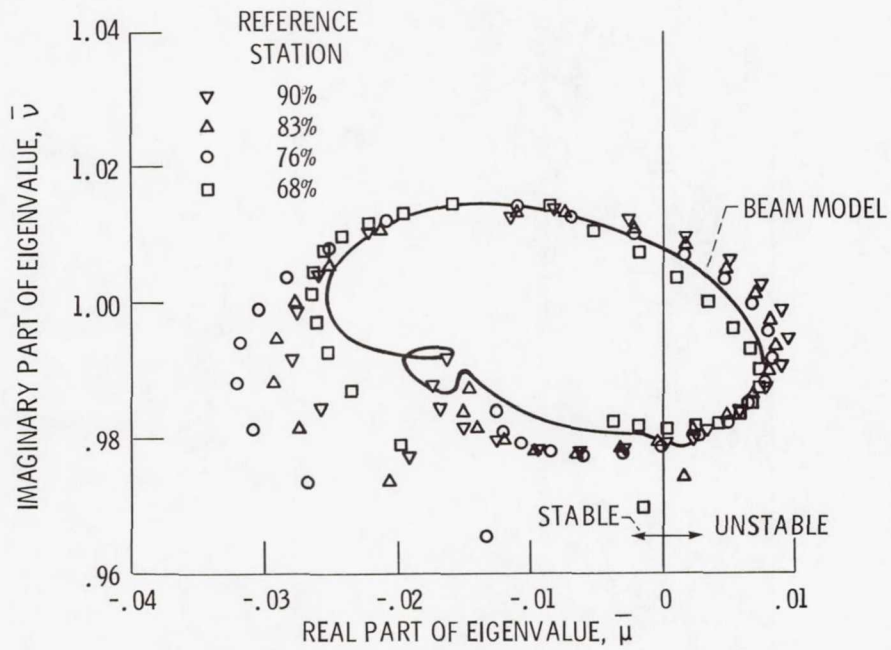


Figure 4. - Comparison of eigenvalues from beam model and typical section models:  $\omega_0 = 1409.6$  rad/sec,  $\Omega = 446.8$  rad/sec,  $M_{ax} = 0.55$ .

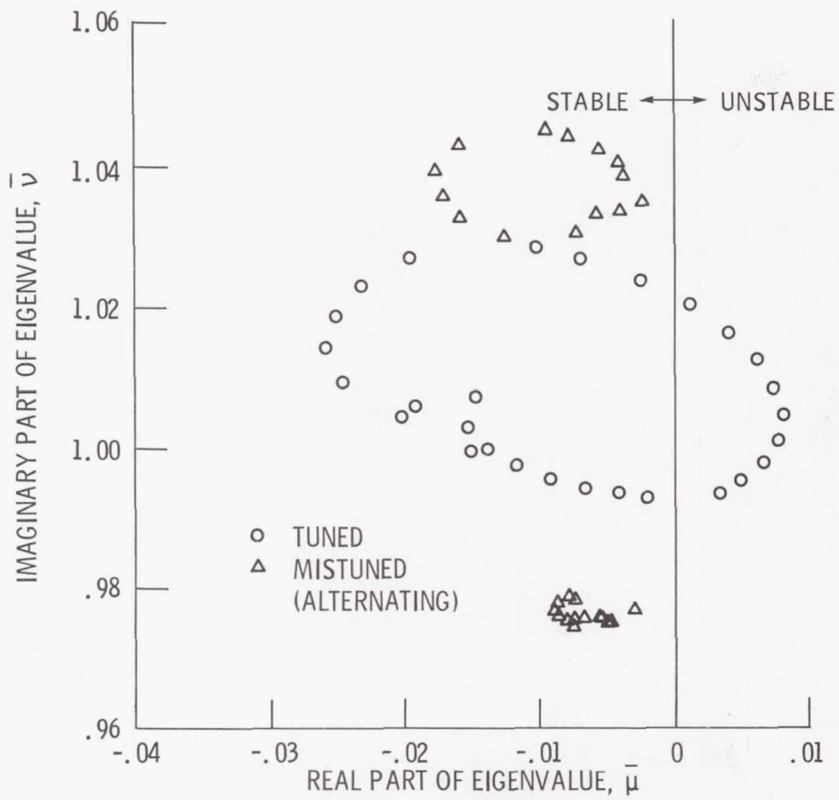


Figure 5. - Comparison of eigenvalues of tuned and mistuned cascade:  $\omega_0 = 1391.1$  rad/sec,  $\Omega = 446.8$  rad/sec,  $M_{ax} = 0.55$ .

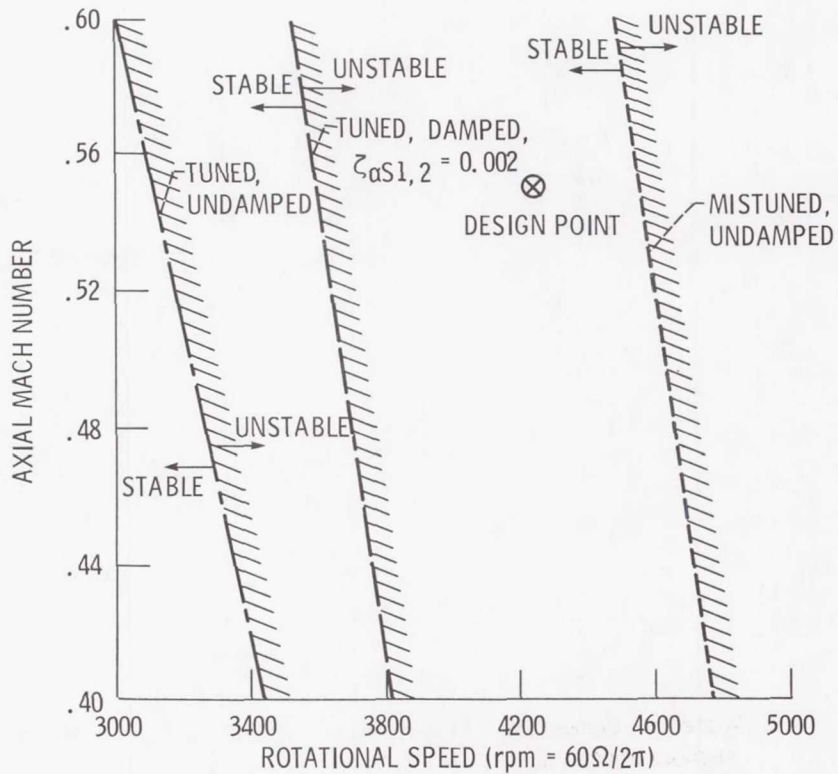


Figure 6. - Comparison of tuned and mistuned flutter boundaries.

1. Report No. NASA TM-82813	2. Government Accession No.	3. Recipient's Catalog No.	
4. Title and Subtitle COUPLED BENDING-BENDING-TORSION FLUTTER OF A MISTUNED CASCADE WITH NONUNIFORM BLADES		5. Report Date	
		6. Performing Organization Code 505-33-52	
7. Author(s) Krishna Rao V. Kaza, The University of Toledo, Toledo, Ohio 43606 and Lewis Research Center and Robert E. Kielb, Lewis Research Center		8. Performing Organization Report No. E-1156	
		10. Work Unit No.	
9. Performing Organization Name and Address National Aeronautics and Space Administration Lewis Research Center Cleveland, Ohio 44135		11. Contract or Grant No. NSG-3139	
		13. Type of Report and Period Covered Technical Memorandum	
12. Sponsoring Agency Name and Address National Aeronautics and Space Administration Washington, D. C. 20546		14. Sponsoring Agency Code	
15. Supplementary Notes Prepared for the Twenty-third Structures, Structural Dynamics, and Materials Conference cosponsored by the AIAA, ASME, ASCE, and AHS, New Orleans, Louisiana, May 10-12, 1982.			
16. Abstract A set of aeroelastic equations describing the motion of an arbitrarily mistuned cascade with flexible, pretwisted, nonuniform blades is developed using an extended Hamilton's principle. The derivation of the equations has its basis in the geometric nonlinear theory of elasticity in which the elongations and shears are negligible compared to unity. A general expression for foreshortening of a blade is derived and is explicitly used in the formulation. The blade aerodynamic loading in the subsonic and supersonic flow regimes is obtained from two-dimensional, unsteady, cascade theories. The aerodynamic, inertial and structural coupling between the bending (in two planes) and torsional motions of the blade is included. The equations are used to investigate the aeroelastic stability and to quantify the effect of frequency mistuning on flutter in turbofans. Results indicate that a moderate amount of intentional mistuning has enough potential to alleviate flutter problems in unshrouded, high-aspect-ratio turbofans.			
17. Key Words (Suggested by Author(s)) Aeroelasticity Cascade flutter Mistuning		18. Distribution Statement Unclassified - unlimited STAR Category 39	
19. Security Classif. (of this report) Unclassified	20. Security Classif. (of this page) Unclassified	21. No. of Pages	22. Price*

\* For sale by the National Technical Information Service, Springfield, Virginia 22161

National Aeronautics and  
Space Administration

Washington, D.C.  
20546

Official Business  
Penalty for Private Use, \$300

SPECIAL FOURTH CLASS MAIL  
BOOK

Postage and Fees Paid  
National Aeronautics and  
Space Administration  
NASA-451



**NASA**

---

POSTMASTER: If Undeliverable (Section 158  
Postal Manual) Do Not Return